Journal of Operation and Automation in Power Engineering

Vol. XX, No. XX, XXXX, Pages: XXXX (Proofed)

http://joape.uma.ac.ir

Research Paper

Impact of Variable DG Penetration on Optimal Distance and Directional Overcurrent Relay Coordination

Raghvendra Tiwari [1, *], *Roshan Chitranshi* [2], and *Devesh Jaiswal* [3]

[1]*Teerthanker Mahaveer University, Moradabad, India.*
[2]*United College of Engineering and Research, Prayagraj, India.*
[3]*United Institute of Technology, Prayagraj, India.*

Abstract— *In contemporary power systems, the hybrid coordination of distance relays (DRs) and directional overcurrent relays (DOCRs) presents challenges due to fluctuating fault current magnitudes and directions caused by the integration of distributed generators (DGs). These fluctuations depend on the type of DG integration, specifically whether it involves inverter-interfaced distributed generators (IIDGs) or synchronous-based distributed generators (SBDGs). SBDG integration can alter the short-circuit level, potentially leading to relay protection miscoordination. Traditional relay protection systems are often ineffective or non-functional in adapting to variable DG penetration, resulting in several protection issues. Therefore, achieving optimal relay coordination is essential to ensure effective protection of microgrid networks under varying levels of DG penetration. This study presents a novel approach for the optimal coordination of hybrid DRs and DOCRs in microgrid environments, considering different levels of DG penetration and employing a modified objective function. The optimal relay settings are determined using Grey Wolf Optimization (GWO) and Genetic Algorithms (GA). Unlike traditional optimization techniques, the GWO algorithm does not require algorithm-specific control parameters, which simplifies implementation. The effectiveness of the proposed method is demonstrated through simulations on the modified IEEE 14-bus test system using MATLAB. The results show improved convergence characteristics, the resolution of local minima issues, minimization of the objective function, and accurate determination of relay operating times, thereby enhancing microgrid protection.*

Keywords—Distance relay, directional overcurrent relay, relay coordination, distributed generation.

1. Introduction

The increasing global energy demand has heightened interest in using renewable energy at consumer locations through distributed generation (DG). Modern power systems require decentralized generation across multiple consumer tiers [1]. Integrating DG into power systems is crucial for the development of electrical networks. The primary benefits of DG include improved reliability, reduced unsupplied energy, lower greenhouse gas emissions, alleviation of congestion in lines and transformers, and decreased overall power losses [2]. Small-scale generation sources can efficiently meet the energy needs of remote regions without requiring substantial investments in new transmission infrastructure. These localized power networks, which integrate their own generation and storage technologies within clearly defined boundaries, are commonly referred to as "microgrids" [3].

Directional overcurrent relays (DOCRs) are widely used as primary protection devices in electrical distribution systems due to their simple operation and low maintenance requirements [4]. In contrast, distance relays (DRs) are primarily employed in transmission and sub-transmission networks because of their faster response times. Within sub-transmission networks, DOCRs are typically applied as backup protection devices due to their comparatively slower operation [5]. In a reliable and effective protection scheme, both primary and backup relays are expected to sense the same fault current simultaneously. However, the primary relay is responsible for operating first to isolate the smallest affected section of the power network. If the primary relay fails to operate, the backup relay activates after a predefined delay known as the coordination time interval (CTI) [6]. The CTI value depends on factors such as relay type and manufacturer specifications. Relay coordination refers to the process of determining the correct operating sequence of all nearby relays when a fault occurs. The operating time of a DOCR is influenced by several parameters, including the Time Multiplier Setting (TMS), Plug Setting (PS), relay characteristic coefficients (λ, η), and the magnitude of the fault current through the relay coil (I_f) [7].

To ensure effective coordination between primary and backup relays, the settings of DOCRs must be meticulously optimized and routinely updated. To minimize relay operating times while maintaining reliability, it is essential to optimize the PS and TMS parameters [8]. Numerous methodologies have been explored in the literature to achieve DOCR coordination. In the late 1990s, traditional optimization techniques were first applied to address relay coordination issues. Linear programming emerged as a significant method, primarily aimed at optimizing TMS only, since the operating time of DOCRs is linearly correlated with TMS [9]. Conventional optimization techniques, including linear

Received: 30 Jan. 2025
Revised: 25 Sept. 2025
Accepted: 21 Oct. 2025
*Corresponding author:
E-mail: raghav.rni@gmail.com (R. Tiwari)
DOI: 10.22098/joape.2025.16657.2285

programming [10], gradient-based methods [11], binary integer programming [12], and sequential quadratic programming [13], exhibit limitations such as susceptibility to local minima, inability to achieve globally optimal solutions, and poor convergence with increasing system size. In a nonlinear programming approach to relay coordination, both TMS and PS are optimized simultaneously [14]. Relay coordination can be formulated as an optimization problem, solvable through either traditional or heuristic techniques. Heuristic algorithms, in particular, have become increasingly popular in protective system studies for resolving relay coordination challenges.

Integrating DGs into the electric grid transforms the radial distribution system into a meshed network, altering short-circuit current characteristics and introducing bidirectional fault currents [15]. These changes may cause overcurrent relays (OCRs) to malfunction. A practical solution is to integrate directional elements into the relays, resulting in directional overcurrent relays (DOCRs) to address these issues [16]. DGs are broadly classified into inverter-interfaced distributed generators (IIDGs) and synchronous-based distributed generators (SBDGs). IIDGs generally have a negligible impact on fault current levels, whereas conventional SBDGs significantly increase fault current magnitudes [17]. Due to variations in fault current magnitudes caused by different levels of DG penetration, existing protection methods and relay coordination may malfunction, leading to unintended tripping. Therefore, it is essential to develop a protection strategy that can adapt to diverse fault current conditions.

The significant integration of DGs has led to elevated fault currents flowing through protection devices. Consequently, switchgear equipment may become inadequate and require costly replacement. Moreover, high fault currents impose considerable stress on power system components such as transformers, lines, and cables during fault conditions. This stress can reduce equipment lifespan, increase failure rates, and ultimately diminish both the reliability and economic viability of the power system [15]. As power systems evolve with high DG penetration, ongoing research focuses on identifying alternative solutions to protection coordination challenges. This underscores the necessity of an adaptive protection scheme capable of autonomously modifying relay settings in response to fluctuating system conditions and operational characteristics [18]. However, a major limitation of adaptive relaying is the requirement for a communication channel, which increases the overall cost of the protection scheme. Additionally, adaptive relaying is vulnerable to cybersecurity threats, which can compromise system reliability.

In the context of distribution networks, several studies have addressed the coordination of DOCRs to mitigate the adverse effects of DG penetration. In [15], the author proposed a DOCR coordination scheme incorporating an optimally sized fault current limiter (FCL) to address the challenges introduced by DG integration. Similarly, in [16], DOCR coordination was achieved using various metaheuristic optimization techniques, including Genetic Algorithm (GA), Gravitational Search Algorithm (GSA), and Particle Swarm Optimization (PSO), under different levels of DG penetration. However, these studies focus exclusively on DOCR coordination. In contrast, in transmission and sub-transmission networks, DRs are typically preferred for primary protection due to their faster operation. In [19], a hybrid coordination strategy involving both DRs and DOCRs was presented, marking a significant advancement. Nevertheless, the proposed approach does not account for the varying impacts of DG penetration on hybrid relay coordination. To address this critical gap, the present study introduces a novel hybrid relay coordination framework that integrates both transmission and distribution networks. The main contributions of this research are summarized as follows:

- A hybrid coordination framework for DRs and DOCRs is proposed to address the protection challenges arising from variable DG penetration in microgrids.
- The study explicitly considers the influence of DG types, including IIDGs and SBDGs, on fault current characteristics and protection coordination performance.
- A modified objective function is formulated to accurately model the coordination problem under varying fault current levels and directions, enhancing relay selectivity and dependability.
- Determination of a common optimal relay setting for both DRs and DOCRs that remains effective across all considered varying DG penetration levels.
- A key innovation of this work lies in its ability to maintain effective hybrid relay coordination without relying on communication-assisted schemes, thereby reducing complexity and potential reliability issues.
- The proposed method is validated through extensive simulations on the modified IEEE 14 bus test system, demonstrating improved convergence behaviour, minimized operating times, and effective mitigation of coordination failures under fluctuating DG scenarios.

Overall, this study presents a robust and adaptive solution to enhance the protection reliability of microgrids with high levels of DG integration, where conventional coordination techniques are often insufficient. The remainder of the paper is organized as follows. Section 1 summarizes previous research in the relevant domain and outlines the contributions of this work. Section 2 discusses the impact of DG penetration on hybrid relay coordination. Section 3 presents the problem formulation and methodology for hybrid relay coordination. Section 4 describes the execution of the test systems, while Section 5 details the implementation of the algorithms and presents the findings. Finally, Section 6 concludes the paper.

2. Impact of variable penetration of DGs on CTI

Hybrid relay coordination involves the coordination of DOCR–DOCR and DOCR–DR pairs. The coordination between these two types of relays, as shown in Fig. 1, is essential for improving selectivity and reliability [20]. The coordination time intervals for DOCR–DOCR and DOCR–DR pairs are represented as CTI and CTI', respectively. To ensure better selectivity using DRs and DOCRs, these CTIs must be maintained.

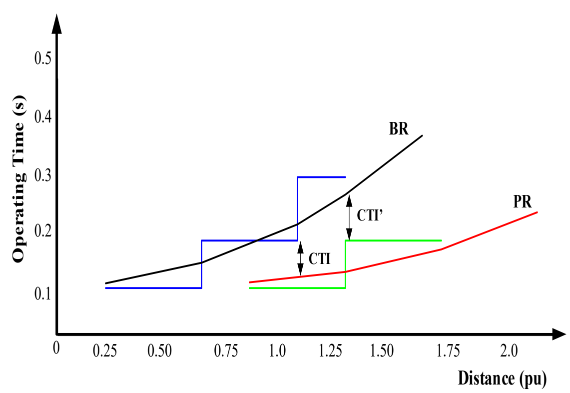

Fig. 1. Hybrid relay coordination between DR and DOCR.

Table 1. Operating modes of modified IEEE-14 bus test system.

Operating Modes (OMs)	Utility grid	DG_1	DG_2	DG_3
OM_1	ON	ON	OFF	OFF
OM_2	ON	OFF	ON	OFF
OM_3	ON	ON	ON	OFF
OM_4	ON	ON	ON	ON

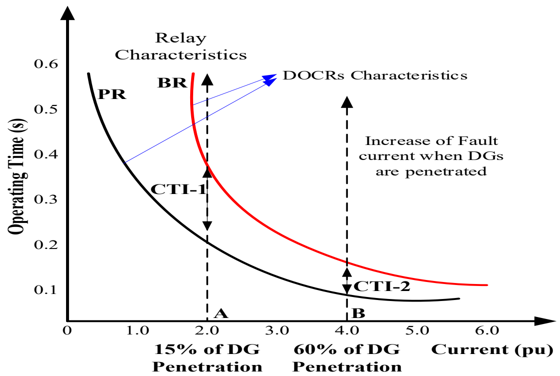

Fig. 2. Impact of variable DG penetration on hybrid relay coordination.

Fig. 2 shows that the CTI decreases from CTI-1 to CTI-2 as DG penetration increases from 15% to 60% [20]. Furthermore, higher penetration levels may violate relay coordination if conventional settings are used. Therefore, a new relay setting approach is required to prevent maloperation under varying levels of DG penetration.

It is also important to note that the impact of DG on transmission and distribution protection coordination depends on the generation type. The contribution of IIDGs to fault current is often minimal and frequently overlooked in coordination studies. The fault contribution of an IIDG typically ranges from 1 to 1.3 times its rated current, depending on its size [17]. Consequently, the rapid proliferation of this category of DGs within power systems necessitates careful consideration, as neglecting their influence could lead to protection system failures. The operational protection of an inverter during a short-circuit event depends on the inverter's voltage conditions. Two scenarios are typically considered when analyzing the fault contribution of IIDGs.

- When the voltage drops below 0.5 pu, the inverter protection activates in less than 0.1s and halts the flow of fault current. In this scenario, it is important to note that the minimum operating time of DOCRs is 0.1 s [21], and thus, no fault current contribution is considered.
- When the voltage exceeds 0.5 pu, the short circuit currents for the coordination issue are determined based on the current contribution of the IIDG, which is equivalent to 1.2 times the rated power of the inverter.

This study presents an optimal coordination strategy for hybrid DOCR-DR protection schemes, considering variable DG penetration. To analyze the impact of different DG integration scenarios, four operating modes (OMs) are defined, as detailed in Table 1. In OM_1 and OM_2, only DG_1 and DG_2 are connected to the system, respectively, while in OM_3, both DG_1 and DG_2 are connected simultaneously. In OM_4, all three DGs (DG_1, DG_2, and DG_3) operate in conjunction with the utility grid. It is important to note that in all operating modes, the utility grid remains continuously connected, restricting the analysis to the grid-connected mode only.

3. Problem Formulation & Methodology

Relay coordination is critical for ensuring adequate system protection, with the goal of isolating only the specific faulty circuit within the network. This is typically achieved through current-based grading systems, time-based grading systems, or a combination of both. In this study, an inverse definite minimum time (IDMT) relay is employed for DOCR coordination, using normal inverse (NI) relay characteristics. The DR and DOCR coordination problem is formulated as an optimization problem with nonlinear constraints. To ensure that each relay operates in the shortest possible time, the objective function must be minimized without allowing miscoordination between relay pairs. The mathematical expression of the objective function incorporates the operating times of primary and backup DOCRs, as well as the second-zone operating times of DRs [22]. The inclusion of backup relay operating times leads to a significant reduction in backup relay operation without violating relay constraints. This study formulates the objective function as follows:

$$OF = \min \left(A_1 \sum_{i=1}^{m} \left(t_{op}^{i}\right)^2 + A_2 \sum_{j=1}^{n} \left(t_{op}^{j} - CTI\right)^2 + \sum_{p=1}^{m} t_{op,z2}^{j} \right) \tag{1}$$

Where,

$$t_{op}^{i} = \frac{\lambda^{i} \times TMS^{i}}{\left[\frac{I_f^i}{PS^i \times CTR^i}\right]^{\eta^i} - 1} \tag{2}$$

In Eq. (1), the first term aims to minimize the total operating time of primary relays to ensure fast fault clearance. The squared formulation penalizes delays more aggressively and enhances overall system responsiveness. The second term ensures proper coordination between primary and backup DOCRs by minimizing deviations from the required CTI, thereby maintaining system selectivity. The third term represents the Zone-2 operating time of DRs, which serve as backup protection if Zone-1 fails or if faults occur beyond the Zone-1 reach. This aspect is particularly important in cases of evolving faults and variations in fault current magnitudes caused by variable DG penetration. The operating time of DOCRs is represented by Eq. (2). To establish adequate DOCR-DR coordination, the optimization problem, as described earlier, must be subject to nonlinear relay constraints, as shown in Eqs. (3)-(4).

$$t_{op,z2}^{j} - t_{op}^{i} \geq CTI' \tag{3}$$

$$t_{op}^{j} - t_{op}^{i} \geq CTI \tag{4}$$

In Eq. (1), m and n are defined as the number of primary and corresponding backup relays. The operating times of i^{th} primary and j^{th} backup DOCRs are represented as t_{op}^{i} and t_{op}^{j} respectively. However, $t_{op,Z2}^{j}$ is the second zone operating time of the corresponding backup DR. The relay settings, TMS^i, PS^i and TMS^j, PS^j are the time multiplier setting and plug setting of i^{th} primary and corresponding j^{th} backup DOCR, respectively. Similarly, the relay characteristics coefficients are assigned as λ^i, η^i and λ^j, η^j for the i^{th} primary and corresponding j^{th} backup DOCR, respectively. According to the IEC-60255 standard, the value of λ and η for NI relay characteristics is 0.14 and 0.02, respectively [23]. The upper and lower bounds on the operating time of a primary DOCR are considered to be 0.1 s and 4 s, respectively [24].

In Eq. (1), the weighting factors were selected using the following procedure. The total relay operating times are calculated based on the different values of A_1 and A_2 such that $A_1 + A_1 = 1$. It has been found that for $A_1 = 0.7$ and $A_2 = 0.3$ the total relay operating time is least. This combination ensures that the system remains fast and stable while preserving coordination integrity even under variable DG conditions [25]. The values were validated through repeated simulations across multiple fault locations and DG penetration levels. This study considers the magnitude of CTI and CTI' between DOCR-DOCR and DOCR-DR relay pairs 0.3s and 0.2s respectively [22]. The maximum load current ($I_{L,\max}^{i}$) is typically considered while choosing the current transformer ratio (CTR). However, CT saturation may occur due to a rise in fault current caused by DG integration. According to [23], the CTR can be computed using the maximum load current ($I^i_{L,\max}$), and the maximum short-circuit current ($I^i_{f,\max}$) flowing through the relay coli to prevent CT saturation, as shown in Eq. (5). The calculated CT ratios (CTRs) for the modified IEEE-14 bus test system using Eq. (5) are shown in Table 2.

$$CTR^i = \max\left(I^i_{L,\max}, \frac{I^i_{f,\max}}{20}\right) \quad (5)$$

Table 2. CT ratio of relays for modified IEEE-14 bus test system.

Relay	CTR	Relay	CTR	Relay	CTR	Relay	CTR
R_1	500	R_9	320	R_{17}	1000	R_{25}	600
R_2	320	R_{10}	240	R_{18}	300	R_{26}	180
R_3	500	R_{11}	320	R_{19}	1000	R_{27}	600
R_4	320	R_{12}	240	R_{20}	300	R_{28}	400
R_5	320	R_{13}	200	R_{21}	800	R_{29}	300
R_6	300	R_{14}	240	R_{22}	700	R_{30}	800
R_7	400	R_{15}	300	R_{23}	400	R_{31}	700
R_8	240	R_{16}	300	R_{24}	300	R_{32}	300

To achieve an optimal hybrid relay coordination, all the decision variables should lie within the pre-specified range given by the relay manufacturer. The upper and lower bounds must be defined for each decision variable as shown in Eqs. (6)-(8).

$$TMS^{i,j}_{\min} \leq TMS^{i,j} \leq TMS^{i,j}_{\max} \quad (6)$$

$$PS^{i,j}_{\min} \leq PS^{i,j} \leq PS^{i,j}_{\max} \quad (7)$$

$$t^j_{\min,\ z2} \leq t^j_{z2} \leq t^j_{z2,\ \max} \quad (8)$$

In this paper, $TMS^{i,j}_{\max}$, $PS^{i,j}_{\max}$ are considered as upper bounds of TMS and PS decision variables for the DOCRs and, similarly, $TMS^{i,j}_{\min}$, $PS^{i,j}_{\min}$ are considered as lower bounds of TMS and PS for the DOCRs. The lower and upper bounds of TMS and PS are set to (0.1–1.1) and (0.5–2.0), respectively [22]. For DRs, Zone-1 operation is assumed to be fixed at 0.01 s. Since the Zone-2 operating time of DRs is variable, it serves as the only decision variable for DRs. For DRs, $t^j_{\min,z2}$ and $t^j_{\max,z2}$ is considered as a lower and upper bound for the second zone operating time. The desired range for the Zone-2 operating time of DRs is (0.3–0.9 s) [22]. The methodology of the proposed protection scheme is illustrated in Fig. 3.

In recent years, the integration of variable DG in distribution networks has introduced nonlinearity, bidirectional fault currents, and system uncertainties, complicating the optimal coordination of protective relays. Traditional analytical techniques often fail to model these nonlinearities effectively. To address such issues, this study employs GA and GWO for optimization, owing to their global search capabilities and robustness in high-dimensional, nonlinear spaces. In this study, GA and GWO are used to determine the optimal relay settings of DOCRs and DRs, which constitutes a nonlinear, multi-objective, and constrained optimization problem. GA is a population-based evolutionary optimization technique inspired by natural selection. It begins with a randomly generated population of relay settings (e.g., TMS, PS, and t_{z2}). Through iterative application of selection, crossover, and mutation, the algorithm evolves these solutions to minimize total operating time, ensure relay coordination constraints, and prevent relay maloperation. GA is well-suited for relay coordination problem because it does not require gradient information and can handle discrete variables and complex constraint formulations [26]. On the other hand, GWO is a recent swarm intelligence algorithm inspired by the social hierarchy and cooperative hunting behavior of grey wolves. In the context of relay coordination, each grey wolf represents a potential set of relay settings. The algorithm uses the three best solutions (alpha-α, beta-β, and delta-δ wolves) to guide the rest of the population (omega-ω wolves) toward optimal coordination settings by simulating encircling, attacking, and searching behaviours [27]. GWO is particularly effective in this application due to its simple structure, minimal tuning parameters, and strong global search capability, making it less prone to premature convergence compared to other algorithms. Unlike traditional methods such as linear programming or sequential quadratic programming, which often require a well-defined, differentiable objective function, GA and GWO can effectively handle nonlinearity, relay coordination inequality constraints, and the discrete nature of the problem. These evolutionary techniques provide a robust and flexible framework for identifying common optimal settings in power systems with variable DG penetration.

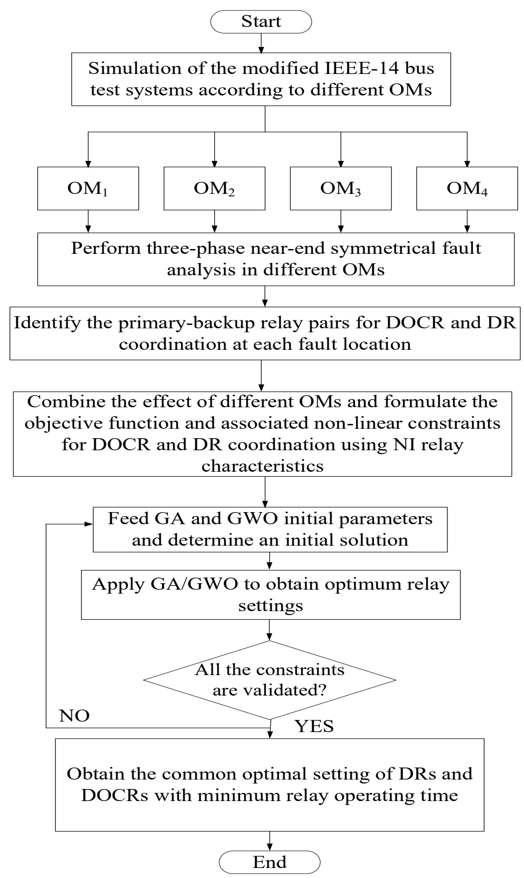

Fig. 3. Proposed methodology of the hybrid protection scheme.

4. Simulation Test case and descriptions

The impact of DG penetration on hybrid coordination between DRs and DOCRs is tested on a modified IEEE-14 bus test system, as shown in Fig. 4 [22]. The system consists of 14 buses ($B_1 - B_{14}$) and 16 lines ($L_1 - L_{16}$). One SBDG (DG_2) with a capacity of 50 MVA is connected at bus B_{13}, while two IIDGs, each with a capacity of 20 MVA, are connected at buses B_{12} and B_{14}. In this test system, the two IIDGs are modelled as wind (DG_1) and solar (DG_3) generating stations. The equivalent internal impedance of each DG is considered to contribute to

Table 3. Primary-backup relay pairs of modified IEEE-14 bus test system.

Sr. No.	Relay pair	Primary relay	Backup relay	Backup distance relay	Sr. No.	Relay pair	Primary relay	Backup relay	Backup distance relay
1	RP_1	R_1	R_4	D_4	32	RP_{32}	R_{12}	R_7	D_7
2	RP_2	R_1	R_8	D_8	33	RP_{33}	R_{12}	R_{15}	D_{15}
3	RP_3	R_2	R_3	D_3	34	RP_{34}	R_{13}	R_5	D_5
4	RP_4	R_2	R_6	D_6	35	RP_{35}	R_{14}	R_9	D_9
5	RP_5	R_2	R_{12}	D_{12}	36	RP_{36}	R_{14}	R_{16}	D_{16}
6	RP_6	R_2	R_{10}	D_{10}	37	RP_{37}	R_{15}	R_9	D_9
7	RP_7	R_3	R_2	D_2	38	RP_{38}	R_{15}	R_{13}	D_{13}
8	RP_8	R_3	R_8	D_8	39	RP_{39}	R_{16}	R_7	D_7
9	RP_9	R_4	R_1	D_1	40	RP_{40}	R_{16}	R_{11}	D_{11}
10	RP_{10}	R_4	R_{12}	D_{12}	41	RP_{41}	R_{17}	R_{20}	D_{20}
11	RP_{11}	R_4	R_{10}	D_{10}	42	RP_{42}	R_{17}	R_{22}	D_{22}
12	RP_{12}	R_4	R_6	D_6	43	RP_{43}	R_{18}	R_{23}	D_{23}
13	RP_{13}	R_5	R_1	D_1	44	RP_{44}	R_{19}	R_{18}	D_{18}
14	RP_{14}	R_5	R_3	D_3	45	RP_{45}	R_{19}	R_{22}	D_{22}
15	RP_{15}	R_5	R_{10}	D_{10}	46	RP_{46}	R_{20}	R_{30}	D_{30}
16	RP_{16}	R_5	R_{12}	D_{12}	47	RP_{47}	R_{21}	R_{18}	D_{18}
17	RP_{17}	R_6	R_{14}	D_{14}	48	RP_{48}	R_{21}	R_{20}	D_{20}
18	RP_{18}	R_7	R_2	D_2	49	RP_{49}	R_{22}	R_{29}	D_{29}
19	RP_{19}	R_7	R_4	D_4	50	RP_{50}	R_{22}	R_{32}	D_{32}
20	RP_{20}	R_8	R_{11}	D_{11}	51	RP_{51}	R_{23}	R_{25}	D_{25}
21	RP_{21}	R_8	R_{15}	D_{15}	52	RP_{52}	R_{24}	R_{17}	D_{17}
22	RP_{22}	R_9	R_1	D_1	53	RP_{53}	R_{25}	R_{28}	D_{28}
23	RP_{23}	R_9	R_3	D_3	54	RP_{54}	R_{26}	R_{24}	D_{24}
24	RP_{24}	R_9	R_6	D_6	55	RP_{55}	R_{27}	R_{26}	D_{26}
25	RP_{25}	R_9	R_{12}	D_{12}	56	RP_{56}	R_{28}	R_{31}	D_{31}
26	RP_{26}	R_{10}	R_{16}	D_{16}	57	RP_{57}	R_{29}	R_{19}	D_{19}
27	RP_{27}	R_{10}	R_{13}	D_{13}	58	RP_{58}	R_{30}	R_{21}	D_{21}
28	RP_{28}	R_{11}	R_1	D_1	59	RP_{59}	R_{30}	R_{32}	D_{32}
29	RP_{29}	R_{11}	R_3	D_3	60	RP_{60}	R_{31}	R_{21}	D_{21}
30	RP_{30}	R_{11}	R_6	D_6	61	RP_{61}	R_{31}	R_{29}	D_{29}
31	RP_{31}	R_{11}	R_{10}	D_{10}	62	RP_{62}	R_{32}	R_{27}	D_{27}

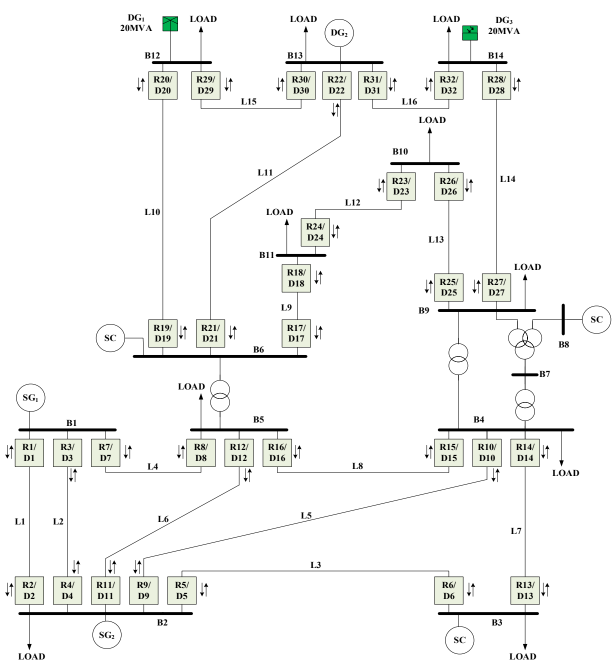

Fig. 4. Single line diagram of modified IEEE-14 bus test system.

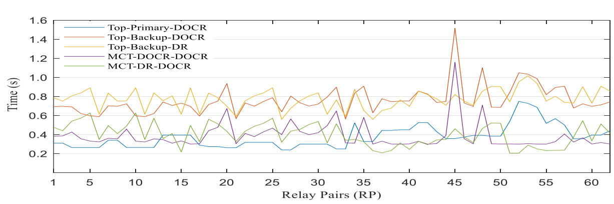

Fig. 5. Primary and backup relay operating times for OM_1 using GWO.

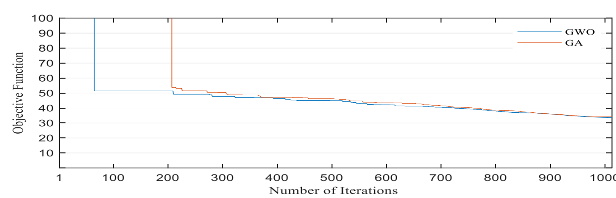

Fig. 6. GA and GWO convergence characteristics for OM_1.

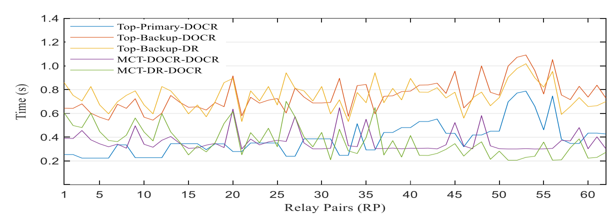

Fig. 7. Primary and backup Relay operating times for OM_2 using GWO.

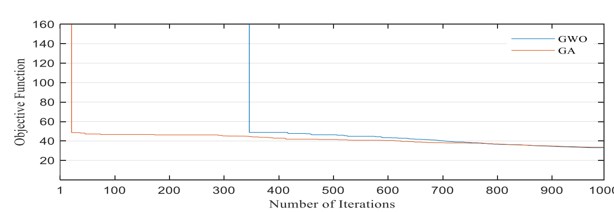

Fig. 8. GA and GWO convergence characteristics for OM_2.

the rated short-circuit MVA during a fault. Additionally, DGs are modelled in the load flow analysis as constant active and reactive power sources based on their ratings and actual power factors. To protect the entire test system, 32 DOCRs and 32 DRs are deployed. Microprocessor-based multifunctional relays are placed at each end of the lines to protect the power system. These relays can operate either as DOCRs or DRs, depending on the fault

Table 4. Near-end three-phase symmetrical fault current for modified IEEE-14 bus test system considering variable penetration of DGs.

Relay pair	OM_1		OM_2		OM_3		OM_4	
	Primary	Backup	Primary	Backup	Primary	Backup	Primary	Backup
RP_1	17.880	2.3531	17.956	2.406	17.964	2.413	17.978	2.425
RP_2	17.880	2.5708	17.956	2.700	17.964	2.713	17.978	2.7375
RP_3	19.094	3.1940	19.328	3.196	19.356	3.196	19.409	3.178
RP_4	19.094	2.9200	19.328	2.953	19.356	2.957	19.409	2.963
RP_5	19.094	3.3042	19.328	3.458	19.356	3.475	19.409	3.504
RP_6	19.094	3.2833	19.328	3.425	19.356	3.442	19.409	3.475
RP_7	17.880	2.3531	17.956	2.406	17.964	2.413	17.978	2.425
RP_8	17.880	2.5708	17.956	2.700	17.964	2.713	17.978	2.7375
RP_9	19.094	3.1940	19.328	3.196	19.356	3.196	19.409	3.196
RP_{10}	19.094	3.3042	19.328	3.458	19.356	3.475	19.409	3.504
RP_{11}	19.094	3.2833	19.328	3.425	19.356	3.442	19.409	3.475
RP_{12}	19.094	2.9200	19.328	2.953	19.356	2.957	19.409	2.963
RP_{13}	19.306	3.0860	19.484	3.086	19.503	3.086	19.541	3.086
RP_{14}	19.306	3.0860	19.484	3.086	19.503	3.086	19.541	3.086
RP_{15}	19.306	2.6208	19.484	2.742	19.503	2.758	19.541	2.788
RP_{16}	19.306	2.7750	19.484	2.908	19.503	2.925	19.541	2.950
RP_{17}	10.523	5.3500	10.593	5.450	10.603	5.463	10.623	5.492
RP_{18}	19.228	2.2969	19.285	2.353	19.293	2.359	19.305	2.369
RP_{19}	19.228	2.2969	19.285	2.353	19.293	2.359	19.305	2.369
RP_{20}	16.783	3.6188	17.417	3.591	17.492	3.588	17.613	3.584
RP_{21}	16.783	6.8367	17.417	6.977	17.492	6.990	17.613	7.053
RP_{22}	19.688	3.1420	19.831	3.146	19.847	3.146	19.875	3.148
RP_{23}	19.688	3.1420	19.831	3.146	19.847	3.146	19.875	3.148
RP_{24}	19.688	2.4067	19.831	2.437	19.847	2.440	19.875	2.450
RP_{25}	19.688	2.4583	19.831	2.608	19.847	2.629	19.875	2.658
RP_{26}	17.404	6.9533	18.017	7.183	18.083	0.287	18.254	7.227
RP_{27}	17.404	5.2600	18.017	5.225	18.083	5.225	18.254	5.210
RP_{28}	19.734	3.1300	19.869	3.136	19.884	3.136	19.919	3.136
RP_{29}	19.734	3.1300	19.869	3.136	19.884	3.136	19.919	3.136
RP_{30}	19.734	2.4933	19.869	2.527	19.884	2.530	19.919	2.540
RP_{31}	19.734	2.4250	19.869	2.567	19.884	2.579	19.919	2.617
RP_{32}	17.408	3.1125	18.088	3.090	18.171	3.088	18.292	3.085
RP_{33}	17.408	6.9267	18.088	7.080	18.171	7.093	18.292	7.163
RP_{34}	16.465	4.3188	16.515	4.350	16.520	4.353	16.530	4.359
RP_{35}	18.200	3.7156	18.821	3.703	18.888	3.703	19.058	3.697
RP_{36}	18.200	7.1400	18.821	7.373	18.888	7.407	19.058	7.420
RP_{37}	12.723	4.3438	13.090	4.356	13.123	4.356	13.277	4.356
RP_{38}	12.723	6.2150	13.090	6.220	13.123	6.220	13.277	6.220
RP_{39}	12.790	3.6500	13.303	3.648	13.373	3.645	13.423	3.648
RP_{40}	12.790	4.4031	13.303	4.406	13.373	4.406	13.423	4.413
RP_{41}	13.471	2.7100	16.397	3.643	16.927	5.123	17.065	5.207
RP_{42}	13.471	1.6629	16.397	6.101	16.927	6.320	17.065	6.486
RP_{43}	11.953	8.9650	11.927	9.395	12.570	9.428	12.827	9.620
RP_{44}	13.316	5.4133	15.904	5.650	16.063	5.663	16.210	5.867
RP_{45}	13.316	1.0300	15.904	5.281	16.063	5.554	16.210	5.694
RP_{46}	13.183	3.4050	13.607	5.103	17.210	4.995	17.320	5.040
RP_{47}	18.101	5.8700	18.691	6.420	19.298	6.423	19.441	6.680
RP_{48}	18.101	2.0500	18.691	3.190	19.298	4.887	19.441	4.973
RP_{49}	5.466	6.6800	16.893	4.300	17.530	5.973	18.019	5.980
RP_{50}	5.466	6.0933	16.893	5.620	17.530	5.633	18.019	6.867
RP_{51}	16.465	10.9767	17.175	11.450	17.225	11.483	17.708	11.805
RP_{52}	16.930	5.0790	18.503	5.551	18.737	5.621	18.843	5.653
RP_{53}	17.445	3.7975	18.378	5.018	18.438	5.090	19.222	6.278
RP_{54}	16.922	10.1533	18.517	11.110	18.722	11.233	18.872	11.323
RP_{55}	16.677	11.1944	17.190	12.667	17.250	12.839	17.300	12.983
RP_{56}	7.000	4.0000	8.840	5.051	8.930	5.103	11.905	5.001
RP_{57}	16.933	3.7830	14.630	4.389	18.627	4.308	18.697	4.330
RP_{58}	9.286	7.1525	17.891	6.063	18.096	6.283	18.456	6.294
RP_{59}	9.286	5.7033	17.891	5.103	18.096	5.133	18.456	6.213
RP_{60}	10.491	6.9175	18.611	5.788	19.167	5.915	19.230	5.971
RP_{61}	10.491	6.1167	18.611	3.950	19.167	5.250	19.230	5.280
RP_{62}	12.323	6.1617	12.700	6.350	12.737	6.368	16.557	6.210

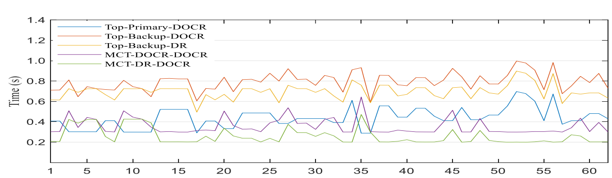

Fig. 9. Primary and backup relay operating times for OM_3 using GWO.

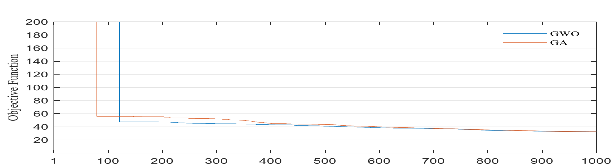

Fig. 10. GA and GWO convergence characteristics for OM_3.

location and relay operating time. Additional details about the test system are provided in [28]. The primary-backup relay pairs

Table 5. Optimal DOCRs and DRs setting for OM_1 using GA and GWO algorithm.

Relay	GWO			GA		
	TMS	PS	t_{z2}	TMS	PS	t_{z2}
R_1	0.1400	0.8387	0.7552	0.1035	1.0110	0.5863
R_2	0.1332	0.6352	0.8360	0.1259	0.5802	0.8247
R_3	0.1745	0.5631	0.8065	0.1613	0.5403	0.6296
R_4	0.1299	0.6944	0.7875	0.1466	0.5015	0.5099
R_5	0.1678	1.0780	0.8742	0.1089	1.8563	0.9402
R_6	0.1035	0.9217	0.8378	0.1003	0.8776	0.6782
R_7	0.1064	1.3679	0.7639	0.1000	1.6261	0.9143
R_8	0.1177	0.8000	0.7515	0.1489	0.5183	0.7918
R_9	0.1213	1.4717	0.6537	0.1257	1.2747	0.7926
R_{10}	0.1004	1.0098	0.6144	0.1137	0.9906	0.7728
R_{11}	0.1108	1.5908	0.6967	0.1169	1.6529	0.8154
R_{12}	0.1067	0.9606	0.8916	0.1449	0.5856	0.8664
R_{13}	0.2588	0.5810	0.6772	0.2212	0.7693	0.6560
R_{14}	0.1335	1.1400	0.6166	0.1533	0.9106	0.5371
R_{15}	0.1914	0.6812	0.5910	0.1174	1.7597	0.6357
R_{16}	0.1378	1.5760	0.5601	0.2334	0.6281	0.8635
R_{17}	0.1515	1.8665	0.9543	0.1430	1.9706	1.0127
R_{18}	0.1184	1.8096	0.7081	0.1284	1.9060	1.0534
R_{19}	0.1097	1.6357	0.7387	0.1706	0.9245	0.7297
R_{20}	0.1570	0.7633	0.8556	0.1236	0.9460	0.8809
R_{21}	0.1276	1.9520	0.7313	0.1767	1.4674	0.9318
R_{22}	0.1261	0.5778	0.8207	0.1411	0.5001	0.9270
R_{23}	0.1812	1.6514	0.7756	0.1902	1.6853	0.8524
R_{24}	0.2351	1.9690	0.9364	0.3140	0.9696	1.1336
R_{25}	0.3822	0.5036	0.7448	0.3649	0.6421	0.8159
R_{26}	0.2614	1.2589	0.7518	0.2193	1.4559	0.7487
R_{27}	0.2591	0.5687	0.8564	0.1515	1.5417	0.8431
R_{28}	0.1123	1.7857	1.0181	0.1143	1.7838	0.9983
R_{29}	0.2613	0.5011	0.9073	0.2419	0.7249	0.6998
R_{30}	0.1025	1.2911	0.7518	0.1014	1.5949	0.8421
R_{31}	0.1002	1.8370	0.8027	0.1247	1.5506	0.9549
R_{32}	0.1292	1.6585	0.9029	0.1247	1.7922	0.6589
OF	33.5797 s			34.4966 s		

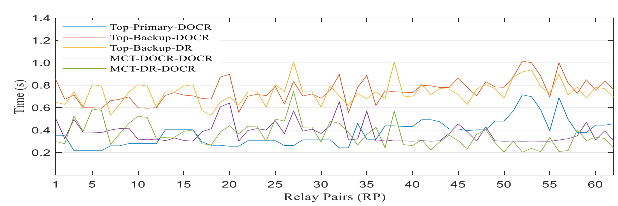

Fig. 11. Primary and backup relay operating times for OM_4 using GWO.

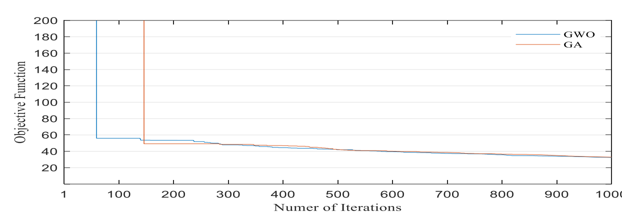

Fig. 12. GA and GWO Convergence Characteristics for OM_4.

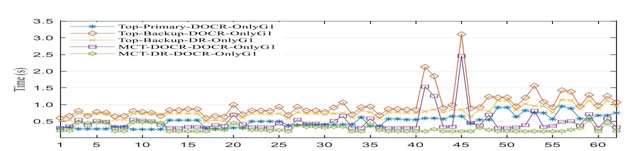

Fig. 13. Primary and backup relay operating time (s) using common optimal relay setting using GWO, considering OM_1 only.

Table 6. Optimal DOCRs and DRs setting for OM_2 using GA and GWO algorithm.

Relay	GWO			GA		
	TMS	PS	t_{z2}	TMS	PS	t_{z2}
R_1	0.1001	1.2251	0.7896	0.1559	0.5281	0.6586
R_2	0.1040	0.8303	0.6980	0.1303	0.6660	0.8172
R_3	0.1718	0.5623	0.7050	0.1347	0.6946	0.7075
R_4	0.1097	0.7403	0.8591	0.1028	0.8018	0.9869
R_5	0.1311	1.4647	0.7761	0.1095	1.6786	0.7086
R_6	0.1098	0.8374	0.8262	0.1159	0.7183	0.6724
R_7	0.1524	0.9515	0.7141	0.1288	1.1471	0.7575
R_8	0.1381	0.6137	0.7522	0.1013	0.8986	0.9981
R_9	0.1505	1.0787	0.6903	0.1033	1.6252	0.6344
R_{10}	0.1064	0.8860	0.5967	0.1570	0.5251	0.6761
R_{11}	0.1703	0.9928	0.8946	0.1068	1.6707	0.6730
R_{12}	0.1082	0.9278	0.6712	0.1179	0.8631	0.5539
R_{13}	0.2409	0.6858	0.8108	0.1774	1.2331	0.7037
R_{14}	0.1007	1.7979	0.5717	0.1011	1.7793	0.5899
R_{15}	0.1716	0.9156	0.5322	0.1181	1.7435	0.5337
R_{16}	0.2193	0.6019	0.9412	0.1674	1.0708	0.6047
R_{17}	0.1687	1.8680	0.9777	0.2012	1.5386	0.9786
R_{18}	0.2204	0.7897	0.7303	0.1772	1.4133	0.8316
R_{19}	0.1956	0.7391	0.5918	0.1458	1.3232	0.7812
R_{20}	0.1001	1.5906	0.7794	0.1540	1.1204	0.9754
R_{21}	0.1693	1.1904	0.6580	0.2700	0.5057	0.8834
R_{22}	0.1465	1.8261	0.7783	0.1823	1.4666	0.8106
R_{23}	0.3486	0.5848	0.8163	0.2714	1.1098	0.8592
R_{24}	0.2991	1.3169	0.9000	0.3554	0.8332	0.8358
R_{25}	0.2624	1.8816	0.9040	0.2771	1.6285	0.8813
R_{26}	0.2789	1.0462	0.8209	0.2970	0.7755	0.7232
R_{27}	0.1874	1.0856	0.6995	0.1388	1.8225	0.8638
R_{28}	0.1970	1.4408	1.0182	0.1839	1.5553	1.0276
R_{29}	0.1363	1.2803	0.6648	0.2231	0.6539	0.7161
R_{30}	0.1404	1.1405	0.5607	0.1850	0.8859	0.7333
R_{31}	0.1423	1.9780	0.9532	0.1532	1.8082	0.9444
R_{32}	0.1182	1.8974	0.7333	0.1299	1.8536	0.7145
OF	33.0877 s			33.3069 s		

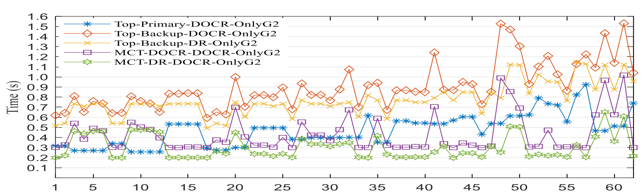

Fig. 14. Primary and backup relay operating time (s) using common optimal relay setting using GWO considering OM_2 only.

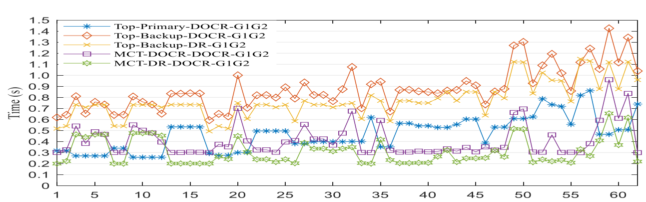

Fig. 15. Primary and backup relay operating time (s) using common optimal relay setting using GWO considering OM_3 only.

Table 7. Optimal DOCRs and DRs settings for OM_3 using GA and GWO algorithm.

Relay	GWO			GA		
	TMS	PS	t_{z2}	TMS	PS	t_{z2}
R_1	0.2146	0.5138	0.7253	0.1178	0.9085	0.8958
R_2	0.1637	0.5006	0.6666	0.1131	0.7185	0.5102
R_3	0.2174	0.5058	0.7251	0.1001	1.1982	0.8823
R_4	0.1621	0.5007	0.6158	0.1230	0.7707	0.7479
R_5	0.2771	0.5410	0.8116	0.1507	1.1812	0.8009
R_6	0.1000	1.0131	0.6891	0.1003	0.9100	0.7313
R_7	0.2210	0.5000	0.6537	0.1270	1.1368	0.8392
R_8	0.1749	0.5000	0.6144	0.1287	0.6637	0.6642
R_9	0.2586	0.5501	0.7595	0.1490	1.0940	0.7384
R_{10}	0.2038	0.5000	0.7253	0.1218	0.8494	0.6682
R_{11}	0.2306	0.5413	0.6694	0.1258	1.4007	0.6597
R_{12}	0.2060	0.5205	0.7244	0.1223	0.8543	0.5837
R_{13}	0.3159	0.5009	0.7588	0.1729	1.2685	0.6844
R_{14}	0.1009	1.7242	0.4949	0.1448	1.0153	0.6172
R_{15}	0.2660	0.5154	0.5934	0.1603	1.0580	0.6564
R_{16}	0.1586	1.1733	0.5868	0.1376	1.6697	0.6911
R_{17}	0.1873	1.5338	0.8978	0.1781	1.8241	0.9948
R_{18}	0.1217	1.9970	0.6266	0.1236	1.9017	0.7068
R_{19}	0.2090	0.5172	0.5796	0.2444	0.5033	0.7455
R_{20}	0.2819	0.5076	0.7354	0.1278	1.8143	0.7767
R_{21}	0.1591	1.4600	0.6837	0.1464	1.5528	0.8022
R_{22}	0.1603	1.6743	0.7346	0.1552	1.7818	0.8501
R_{23}	0.1887	1.6881	0.6568	0.1999	1.5245	0.7874
R_{24}	0.2288	1.9800	0.8063	0.3746	0.7663	0.8767
R_{25}	0.2287	1.8279	0.7555	0.3246	0.9176	0.8080
R_{26}	0.2145	1.6435	0.6246	0.3397	0.5493	0.6406
R_{27}	0.1390	1.7112	0.6335	0.1550	1.4741	0.7081
R_{28}	0.1782	1.4436	0.8766	0.1528	1.8363	0.9572
R_{29}	0.1232	1.9781	0.6837	0.1728	1.2742	0.6825
R_{30}	0.1536	1.4136	0.7408	0.1729	0.9542	0.6825
R_{31}	0.1855	1.3828	0.8728	0.1618	1.6153	0.8875
R_{32}	0.1169	1.9688	0.6717	0.1155	1.9861	0.7800
OF	32.3696 s			32.5443 s		

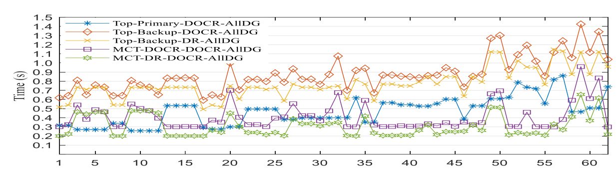

Fig. 16. Primary and backup relay operating time (s) using common optimal relay setting using GWO considering OM_4 only.

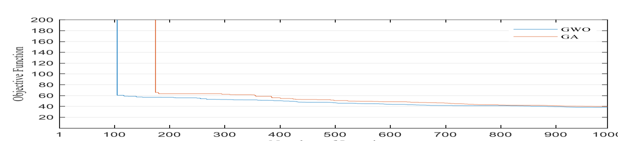

Fig. 17. Convergence characteristics of GA and GWO using common optimal relay settings.

for the modified IEEE-14 bus test system are shown in Table 3. Table 3 indicates that 62 relay pairs (RPs), comprising various combinations of primary and backup relays, are formed to protect the entire electrical network. For RP_1, the primary DOCR is R_1, and the corresponding backup DOCR and DR are R_4 and D_4, respectively. Similar configurations of primary and backup relay pairs, depending on the fault location, can also be found in Table 3.

5. Results and Discussions

This section describes the hybrid relay coordination of DOCRs and DRs using GA and GWO algorithms. The analysis of a

Table 8. Optimal DOCRs and RDs settings for OM_4 using GA and GWO algorithm.

Relay	GWO			GA		
	TMS	PS	t_{z2}	TMS	PS	t_{z2}
R_1	0.1836	0.5218	0.7398	0.1152	1.1308	0.7047
R_2	0.1001	0.8506	0.5334	0.1622	0.5000	0.6109
R_3	0.1056	1.1382	0.7414	0.2004	0.5451	0.7110
R_4	0.1293	0.8492	0.6489	0.1663	0.5000	0.6335
R_5	0.1883	0.8273	0.7251	0.2477	0.6546	0.8113
R_6	0.1102	0.8321	0.6070	0.1001	1.0473	0.6734
R_7	0.1020	1.3983	0.7038	0.2203	0.5192	0.6817
R_8	0.1148	0.8437	0.6291	0.1687	0.5049	0.5884
R_9	0.1162	1.4901	0.6808	0.1220	1.5879	0.7430
R_{10}	0.1168	0.8954	0.7930	0.2001	0.5001	0.7012
R_{11}	0.1224	1.3922	0.6950	0.2428	0.5192	0.6759
R_{12}	0.1001	1.1036	0.8046	0.2047	0.5000	0.7319
R_{13}	0.1750	1.2257	1.0075	0.3093	0.5000	0.7385
R_{14}	0.1101	1.7965	0.5731	0.1954	0.6154	0.5539
R_{15}	0.1945	0.6523	0.6223	0.2330	0.6997	0.6054
R_{16}	0.1258	1.8275	0.7435	0.1337	1.9336	0.5984
R_{17}	0.1562	1.9481	0.9185	0.1819	1.5994	0.8961
R_{18}	0.1395	1.7035	0.7654	0.1225	1.9991	0.6420
R_{19}	0.1613	1.1133	0.7149	0.2070	0.6322	0.6420
R_{20}	0.1393	1.5607	0.8062	0.2342	0.7475	0.7326
R_{21}	0.1512	1.5013	0.7812	0.1335	1.9773	0.7368
R_{22}	0.1850	1.3041	0.7161	0.1425	1.9737	0.7267
R_{23}	0.1928	1.7535	0.7707	0.1763	1.9151	0.6582
R_{24}	0.2863	1.2315	0.7896	0.2285	1.9906	0.8075
R_{25}	0.2532	1.6131	0.8724	0.2569	1.4598	0.7483
R_{26}	0.2004	1.7949	0.7278	0.2451	1.1975	0.6057
R_{27}	0.1242	1.9976	0.6931	0.1265	1.9901	0.6695
R_{28}	0.2100	1.4747	0.9356	0.1810	1.7512	0.8842
R_{29}	0.2309	0.7961	0.7700	0.1735	1.2592	0.7360
R_{30}	0.1417	1.4351	0.6292	0.2538	0.5844	0.7320
R_{31}	0.1593	1.6614	0.8982	0.2469	0.8348	0.8570
R_{32}	0.1429	1.9388	0.6851	0.1648	1.4964	0.6994
OF	31.8781 s			32.0272 s		

near-end three-phase fault in the modified IEEE-14 bus test system is presented in Table 4, covering all operational modes: OM_1, OM_2, OM_3, and OM_4. For RP_1, the primary relay coil currents are 17.880 A, 17.956 A, 17.964 A, and 17.978 A in OM_1, OM_2, OM_3, and OM_4, respectively. Similarly, the corresponding backup relay coil currents are 2.3531 A, 2.406 A, 2.413 A, and 2.425 A in OM_1, OM_2, OM_3, and OM_4, respectively. The analysis of fault currents shows that an increase in DG penetration within the electrical power network correlates with a rise in fault current magnitude.

The result discussion section is further divided into five subsections i.e.,

- When only DG_1 connected i.e., OM_1
- When only DG_2 connected i.e, OM_2
- When both DG_1 and DG_2 connected i.e., OM_3
- When all DGs (DG_1, DG_2 and DG_3) connected i.e., OM_4
- Common operating modes

5.1. Only DG_1 connected i.e., OM_1

In OM_1, only DG_1 is connected to the system along with the utility grid. The near-end fault current magnitude at each location, as measured through each relay coil, is provided in Table 4. A comprehensive analysis of the optimal relay settings for DOCRs and DRs is presented in Table 5. According to the results, the optimal objective function value is 33.5797 s using GWO and 34.4966 s using GA. For OM_1, the primary and backup relay operating times, shown in Fig. 5, are derived from the optimal relay settings listed in Table 5. The results indicate that the backup relay operating time is greater than that of the corresponding primary relay across all relay pairs (RP_1-RP_{62}). Furthermore, the measured coordination time (MCT) for DOCR-DOCR coordination and MCT' for DOCR–DR coordination exceed the predefined CTI and CTI' between the primary and corresponding backup relays. Here, MCT is defined as the actual obtained time gap between the primary and corresponding backup relay. The convergence characteristics of GA and GWO for OM_1 are shown in Fig. 6, which demonstrates that the GWO algorithm requires fewer iterations to achieve the optimal objective function value compared to GA.

5.2. Only DG_2 connected i.e., OM_2

In this section, the hybrid relay coordination analysis is discussed for OM_2. In OM_2, the system is connected to DG_2 in conjunction with the utility grid. The magnitude of the near-end fault current at each location, flowing through each relay coil, is provided in Table 4. The optimal relay settings of DOCRs and DRs are thoroughly analyzed and presented in Table 6. The results indicate that the optimal objective function values are 33.0877 s and 33.3069 s, achieved through GWO and GA, respectively. These values are lower than those obtained in OM_1, which can be explained by the relay inverse characteristics, as the fault current magnitude in OM_2 is greater than in OM_1. Within the framework of OM_2, the operating times for both primary and backup relays, illustrated in Fig. 7, are determined using the optimal relay configurations outlined in Table 6. The findings show that the operating time of the backup relay exceeds that of the corresponding primary relay across all relay pairs (RP_1-RP_{62}). Furthermore, the MCT for DOCR–DOCR coordination and the MCT' for DOCR–DR coordination exceed the predefined thresholds between the primary and backup relays, thereby validating the essential criteria for effective optimal relay coordination. The convergence characteristics of GA and GWO for OM_2 are illustrated in Fig. 8, which demonstrates that the GWO algorithm requires fewer iterations to reach the optimal objective function value compared to GA.

5.3. Both DG_1 and DG_2 connected i.e., OM_3

Similarly, a detailed evaluation of DOCR and DR coordination under OM_3 is presented in Table 7. The obtained results show that all relay settings derived using GWO and GA for DOCRs and DRs lie within their respective desired ranges. The optimal objective function values achieved using GWO and GA are 32.3696 s and 32.5443 s, respectively. Due to the higher penetration of DGs in the system, the results indicate that the total relay operating times in OM_3 are lower compared to OM_1 and OM_2. Fig. 9 illustrates the operating times of primary and backup relays for GWO under OM_3. The findings confirm that, for all relay pairs (RP_1-RP_{62}), the backup relay operating times consistently exceed those of the corresponding primary relays. Additionally, the measured coordination time (MCT) for both DOCR–DOCR and DOCR–DR coordination surpasses the minimum required time gap between the primary and backup relays. Fig. 10 depicts the convergence characteristics of GWO and GA under OM_3, showing that GWO achieves the optimal objective function value in fewer iterations compared to GA.

5.4. All DGs are connected, i.e., OM_4

A detailed evaluation of DOCR-DR coordination under OM_4 is presented in Table 8. All optimal relay settings obtained via GWO and GA fall within the desired ranges of their respective decision variables. The optimal objective function values are 31.8781 s and 32.0272 s when using GWO and GA, respectively. Fig. 11 illustrates the primary and backup relay operating times obtained through GWO under OM_4. The results show that, for all relay pairs, the backup relay operating time exceeds that of the corresponding primary relay. Furthermore, the measured coordination time (MCT) for both DOCR–DOCR and DOCR–DR coordination surpasses the required time gap between the primary and backup relays. It can also be concluded that the optimal objective function value is lowest when all DGs are connected. This

Table 9. Summary of relay constraint violations using GWO.

Operating Modes (OMs)	Network Configuration	Constraint Configuration	Existing Constraints	OM_1	OM_2	OM_3	OM_4
OM_1	Only DG_1 connected	Top-Prim-DOCR	32	0	0	0	0
		CTI-DOCR-DOCR	62	0	13	13	12
		CTI-DR-DOCR	62	0	0	0	0
OM_2	Only DG_2 connected	Top-Prim-DOCR	32	0	0	0	0
		CTI-DOCR-DOCR	62	8	0	12	8
		CTI-DR-DOCR	62	6	0	0	0
OM_3	Only DG_1 and DG_2 connected	Top-Prim-DOCR	32	0	0	0	0
		CTI-DOCR-DOCR	62	10	4	0	5
		CTI-DR-DOCR	62	16	3	0	0
OM_4	All DGs connected	Top-Prim-DOCR	32	0	0	0	0
		CTI-DOCR-DOCR	62	7	3	3	0
		CTI-DR-DOCR	62	11	4	2	0
All OMs	–	Top-Prim-DOCR	32	0	0	0	0
		CTI-DOCR-DOCR	62	0	0	0	0
		CTI-DR-DOCR	62	0	0	0	0

Table 10. Common optimal DRs and DOCRs settings for all OMs using GWO and GA.

Relay	GWO			GA		
	TMS	PS	t_{z2}	TMS	PS	t_{z2}
R_1	0.1341	1.0134	0.7334	0.2140	0.5205	0.7199
R_2	0.1464	0.5000	0.5396	0.1754	0.5000	0.6775
R_3	0.1505	0.8852	0.7339	0.2189	0.5001	0.7203
R_4	0.1378	0.5187	0.5167	0.1753	0.5003	0.6873
R_5	0.2880	0.5084	0.8188	0.2378	0.5007	0.6535
R_6	0.1000	1.0228	0.7103	0.1928	0.5016	0.7204
R_7	0.1000	1.6174	0.7492	0.2586	0.5010	0.7949
R_8	0.1578	0.5000	0.5393	0.1000	1.0350	0.6148
R_9	0.2650	0.5369	0.7689	0.2633	0.5000	0.7348
R_{10}	0.1974	0.5437	0.7338	0.1968	0.5000	0.7210
R_{11}	0.1688	1.1165	0.7494	0.2838	0.5001	0.7940
R_{12}	0.2114	0.5133	0.7334	0.1895	0.5033	0.6830
R_{13}	0.3192	0.5062	0.7689	0.1434	1.8928	0.7362
R_{14}	0.1608	0.8481	0.4925	0.1894	0.9178	0.6298
R_{15}	0.2691	0.5183	0.6045	0.2540	0.5101	0.5623
R_{16}	0.2504	0.5827	0.5840	0.2738	0.5623	0.6298
R_{17}	0.1661	1.9569	1.0238	0.2134	1.4814	1.0419
R_{18}	0.1568	1.8039	0.8500	0.1457	1.9965	0.8765
R_{19}	0.2287	1.2069	1.1296	0.2508	1.0644	1.1215
R_{20}	0.1274	1.7856	0.7916	0.2267	0.9126	0.8609
R_{21}	0.1763	1.9819	0.8751	0.1783	1.9891	0.8850
R_{22}	0.3191	0.5042	0.8500	0.3363	0.5002	0.8784
R_{23}	0.1970	1.9707	0.7692	0.2543	1.2343	0.7596
R_{24}	0.2631	1.9054	0.9503	0.2633	1.9857	0.9730
R_{25}	0.2485	1.8224	0.8350	0.3176	1.1986	0.8686
R_{26}	0.2484	1.7611	0.7632	0.2901	1.3118	0.7755
R_{27}	0.1753	1.9816	0.9578	0.1795	1.9753	0.9747
R_{28}	0.2155	1.4619	0.9554	0.1803	1.9739	1.0074
R_{29}	0.4613	0.5008	1.1224	0.4059	0.7360	1.1602
R_{30}	0.2463	0.5068	0.6363	0.2499	0.7119	0.7777
R_{31}	0.1814	1.6590	1.1484	0.1870	1.6124	1.1838
R_{32}	0.2053	1.8917	1.1194	0.2090	1.9338	1.1602
OF	38.1993 s			39.9635 s		

outcome can be attributed to the highest fault current magnitude in OM_4, which results in the shortest total relay operating time. Fig. 12 depicts the convergence characteristics of GA and GWO for OM_4, demonstrating that the GWO algorithm achieves the optimal objective function value in fewer iterations compared to GA.

Based on the discussion above, a different set of relay settings is required to achieve optimal hybrid relay coordination for each OM. In other words, the optimal relay settings derived for one OM cannot be applied to another OM due to changes in fault current magnitude. This subsection estimates the number of relay constraint violations that occur when a set of optimal relay settings from one OM is applied to different OMs. The following events are considered relay constraint violations if:

- The magnitudes of MCT and MCT' are less than 0.3 s and 0.2 s, respectively, for the corresponding primary-backup relay pairs.
- The backup relay operates before the primary relay.
- The primary DOCR operates in less than 0.11 s after the fault occurrence.

Table 11. Comparative analysis of hybrid relay coordination for the modified IEEE-14 bus test system.

Operating Modes (OMs)	OM_1	OM_2	OM_3	OM_4	Considered All OMs
GA	34.4966 s	33.3069 s	32.5443 s	32.0272 s	39.9635 s
GWO	33.5797 s	33.0877 s	32.3696 s	31.8781 s	38.1993 s
% reduction in OF	2.73%	0.67%	0.54%	0.46%	4.61%

Table 9 presents a summary of constraint violations that occur when relay settings derived from one OM are applied to different OMs using GWO. From Table 9, it can be observed that when the relay settings obtained for OM_1 using GWO are applied to OM_2, OM_3, and OM_4, the number of relay constraint violations is 13, 13, and 12, respectively. Similarly, when the relay settings obtained for OM_2 using GWO are applied to OM_1, OM_3, and OM_4, the number of violations is 8, 12, and 8, respectively. Similar findings can be observed for the other OMs. However, when a common optimal relay setting is applied to any OM, no constraint violations occur.

Therefore, to determine a common optimal relay setting that can be applied across all considered OMs, the impact of variable DG penetration must be considered simultaneously. The derived common optimal relay settings for hybrid DOCR-DR coordination are presented in Table 10. According to Table 10, the optimal objective function value is highest when the effects of all OMs are considered, due to the large number of nonlinear constraints associated with the optimization problem. The optimal objective function values obtained using GWO and GA are 38.1993 s and 39.9635 s, respectively. The results further demonstrate that, for each OM, the GWO algorithm yields better performance than GA. Figs. 13-16 show the primary and corresponding backup relay operating times for OM_1, OM_2, OM_3, and OM_4, respectively, using the common optimal relay settings obtained via GWO. As seen in the figures, for all relay pairs, the backup relay operating time exceeds that of the corresponding primary relay, and the magnitudes of MCT and MCT' consistently surpass the specified CTI.

A comparative analysis of hybrid relay coordination between DOCRs and DRs using GWO and GA is presented in Table 11. The findings indicate that GWO performs better than GA for hybrid relay coordination problems. Furthermore, the modified objective function promotes improved coordination between primary and backup relays, thereby enhancing the reliability of microgrids. As a result, the proposed method demonstrates greater accuracy, adaptability, and efficiency, as reflected in the results. According to Table 11, the objective function value in OM_1 is 34.4966 s using GA and 33.5797 s using GWO. Similarly, in OM_2, OM_3, and OM_4, the total relay operating times obtained using GA are 33.3069 s, 32.5443 s, and 32.0272 s, respectively, while GWO yields 33.0877 s, 32.3696 s, and 31.8781 s. These results show a consistent reduction in total relay operating time from OM_1 to OM_4, attributed to increasing DG penetration, which aligns with the inverse time-current characteristics of DOCRs. The total relay operating time is highest when accounting for variable DG penetration, which can be attributed to the increased number of relay coordination constraints in this operating mode. The percentage reduction in total relay operating time using GWO compared to GA is 2.73%, 0.67%, 0.54%, and 0.46% in OM_1, OM_2, OM_3, and OM_4, respectively. In the common operating mode, the reduction in total relay operating time is 4.61% when using GWO compared to GA.

6. CONCLUSION

The variable penetration of DG may lead to changes in fault current magnitude and affect the coordination of hybrid DR-DOCR. Due to these variations in fault current magnitude, selectivity constraints may be violated, resulting in maloperation of relays. In this study, the impact of variable DG penetration on hybrid relay coordination is considered, and a common optimal relay setting is determined that can be applied across all the considered operating modes (OMs). The proposed protection scheme is tested on a modified IEEE-14 bus test system, with optimal relay settings determined using two metaheuristic optimization techniques: GA and GWO. The results show that the magnitude of the objective function (OF) is 39.9635 s and 38.1993 s when using GA and GWO, respectively, while considering the impact of variable DG penetration. From the results, it can be concluded that the proposed protection scheme not only maintains all selectivity constraints under DG penetration uncertainty but also achieves a significant reduction in total relay operating times. The primary findings of this study are as follows:

- Investigated hybrid relay coordination in a modified IEEE-14 bus system under multiple DG (both SBDG and IIDG) penetration levels.
- Applied GWO with a modified objective function, which includes the second zone operating times of DRs, to determine common relay settings suitable across all operating modes (OMs).
- GWO outperforms GA in terms of minimizing the total relay operating time across all scenarios. It consistently yields the lowest objective function values in each OM.
- Improved CTI performance using the modified objective function results in fewer miscoordination cases.
- The proposed protection scheme enhances primary-backup relay coordination, improving system reliability in microgrids.

The primary limitation of this study is that the obtained optimal relay settings are applicable only to the operating modes (OMs) considered here. These settings may not be valid for other DG penetration levels or in islanded mode operations. For future work, the proposed protection scheme can be evaluated using more recent metaheuristic optimization techniques on larger power systems. Additionally, to further improve reliability, the islanded mode of operation and other DG penetration levels may also be considered.

ACKNOWLEDGEMENT

The authors acknowledge the use of artificial intelligence tools (e.g., ChatGPT by OpenAI) for language editing and clarity improvement during the preparation of this manuscript. The authors are fully responsible for the scientific content, analysis, and conclusions.

REFERENCES

[1] L. Abu-El-Haija, B. E. Layan, Y. Refai, M. K. Alsafadi, M. J. Abdel-Rahman, and A. I. Abu-El-Haija, "Multi-microgrid system optimization addressing the uncertainties in generation and load demand," *IEEE Access*, vol. 13, pp. 62165–62178, 2025.

[2] G. V. Ramos, D. Brandao, T. M. Parreiras, D. I. Brandao, and B. d. J. C. Filho, "A zero harmonic distortion master converter for medium voltage microgrids," in *Proc. IEEE Appl. Power Electron. Conf. Expo.*, pp. 1355–1362, 2025.

[3] G. Meena, V. P. Meena, A. Mathur, V. P. Singh, A. T. Azar, and I. A. Hameed, "Optimizing power flow and stability in hybrid AC/DC microgrids: AC, DC, and combined analysis," *Math. Comput. Appl.*, vol. 29, no. 6, p. 108, 2024.

[4] H. Shad, M. Gandomkar, and J. Nikoukar, "An improved optimal protection coordination for directional overcurrent relays in meshed distribution networks with dg using a novel truth table," *J. Oper. Autom. Power Eng.*, vol. 11, no. 3, pp. 151–161, 2023.

[5] M. Abdelhamid, S. Kamel, and A. Korashy, "An adaptive protection scheme for coordination of distance and directional overcurrent relays in distribution systems based on a modified school-based optimizer," *Electronics*, vol. 10, no. 21, p. 2628, 2021.

[6] S. D. Godwal, K. S. Pandya, S. C. Vora, C. R. Mehta, and V. R. Rajput, "Optimal overcurrent relay coordination for interconnected power systems: A proper approach and improved technique," *e-Prime Adv. Electr. Eng. Electron. Energy*, vol. 5, pp. 1–10, 2023.

[7] Y. González and A. Conde, "New overcurrent relay coordination method through time intervals to enhance microgrid protection," *IEEE Access*, vol. 9, pp. 166792–166803, 2021.

[8] P. Niranjan, N. K. Choudhary, N. Singh, and R. K. Singh, "Optimal coordination of dual-setting directional over current relay in microgrid considering multi-parametric characteristics," *J. Oper. Autom. Power Eng.*, vol. 13, no. 2, pp. 174–183, 2025.

[9] S. Biswal and S. R. Samantaray, "Relay coordination scheme in microgrids based on non-standard tripping curve of DOCRs with multiple setting groups," *IEEE Trans. Ind. Informat.*, vol. 20, no. 4, pp. 5737–5749, 2024.

[10] D. Alcala-Gonzalez, E. M. Garcia del Toro, M. I. Mas-Lopez, S. Garcia-Salgado, and S. Pindado, "Linear programming coordination for overcurrent relay in electrical distribution systems with distributed generation," *Appl. Sci.*, vol. 12, no. 9, pp. 1–16, 2022.

[11] R. M. Rizk-Allah and A. A. El-Fergany, "Effective coordination settings for directional overcurrent relay using hybrid gradient-based optimizer," *Appl. Soft Comput.*, vol. 112, 2021.

[12] R. Correa, G. Cardoso, O. C. B. de Araujo, and L. Mariotto, "Online coordination of directional overcurrent relays using binary integer programming," *Electr. Power Syst. Res.*, vol. 127, pp. 118–125, 2015.

[13] S. K. ElSayed and E. E. Elattar, "Hybrid harris hawks optimization with sequential quadratic programming for optimal coordination of directional overcurrent relays incorporating distributed generation," *Alex. Eng. J.*, vol. 60, no. 2, pp. 2421–2433, 2021.

[14] A. Bayazidi, A. Abdali, and J. C. Vasquez, "Optimal coordination of directional overcurrent relays in power energy systems with emphasis on the discreteness of variables: Comprehensive comparisons," *Heliyon*, vol. 10, no. 19, 2024.

[15] M. S. Kandil, A. Elmitwally, E. Gouda, and A. Amer, "Mitigation of DGs impact on variable-topology meshed network protection system by optimal fault current limiters considering overcurrent relay coordination," *Electr. Power Syst. Res.*, vol. 186, 2020.

[16] D. M. Bui, P. D. Le, T. P. Nguyen, and H. Nguyen, "An adaptive and scalable protection coordination system of overcurrent relays in distributed-generator-integrated distribution networks," *Appl. Sci.*, vol. 11, no. 8, pp. 1–43, 2021.

[17] N. Nimpitiwan, G. T. Heydt, R. Ayyanar, and S. Suryanarayanan, "Fault current contribution from synchronous machine and inverter based distributed generators," *IEEE Trans. Power Deliv.*, vol. 22, no. 1, pp. 634–641, 2007.

[18] C. Plongkrathok, K. Kaiyawong, and K. Chayakulkheeree, "Adaptive directional overcurrent relay coordination in microgrid considering optimal full setting parameters," *Electr. Power Components Syst.*, vol. 52, no. 7, pp. 985–1000, 2023.

[19] A. E. L. Rivas, L. A. G. Pareja, and T. Abrao, "Coordination of distance and directional overcurrent relays using an extended continuous domain ACO algorithm and an hybrid ACO algorithm," *Electr. Power Syst. Res.*, vol. 170, pp. 259–272, 2019.

[20] D. K. Singh, S. Sarangi, A. K. Singh, and S. R. Mohanty, "Coordination of dual-setting overcurrent and distance relays for meshed distribution networks with distributed generations and dynamic voltage restorer," *Smart Sci.*, vol. 11, no. 1, pp. 135–153, 2022.

[21] H. Saberi and T. Amraee, "Coordination of directional over-current relays in active distribution networks using generalised benders decomposition," *IET Gener. Transm. Distrib.*, vol. 11, no. 16, pp. 4078–4086, 2017.

[22] R. Tiwari, R. K. Singh, and N. K. Choudhary, "Enhanced combined protection scheme using dual setting directional overcurrent and distance relays considering severe line contingencies," *Electr. Power Components Syst.*, pp. 1–22, 2023.

[23] R. Tiwari, R. K. Singh, and N. K. Choudhary, "Coordination of dual setting overcurrent relays in microgrid with optimally determined relay characteristics for dual operating modes," *Prot. Control Mod. Power Syst.*, vol. 7, no. 1, pp. 1–18, 2022.

[24] R. Tiwari, R. K. Singh, and N. K. Choudhary, "Optimal relay coordination for dg-based power system using standard and user-defined relay characteristics," *Int. J. Eng. Technol. Innov.*, vol. 12, no. 3, pp. 207–224, 2022.

[25] M. N. Alam, A. Sallem, and N. Masmoudi, "Protection coordination using mixed characteristics of directional over-current relays in interconnected power distribution networks," in *Proc. IEEE Int. Energy Conf.*, pp. 761–766, 2020.

[26] S. Katoch, S. S. Chauhan, and V. Kumar, "A review on genetic algorithm: past, present, and future," *Multimed. Tools Appl.*, vol. 80, pp. 8091–8126, 2021.

[27] S. N. e. a. Makhadmeh, "Recent advances in Grey Wolf optimizer, its versions and applications: Review," *IEEE Access*, vol. 12, pp. 22991–23028, 2024.

[28] R. Christie, "Power system test cases," 1993. Available from: http://www.ee.washington.edu/research/pstca.